Wigner 6j symbols for SU(N): Symbols with at least two quark-lines

Judith Alcock-Zeilinger, 1, 2 Stefan Keppeler, 2 Simon Plätzer, 3, 4, 1 and Malin Sjodahl 5, 1

- 1) Erwin Schrödinger Institute for Mathematics and Physics, University of Vienna, Boltzmanngasse 9, A-1090 Wien, Austria
- ²⁾ Fachbereich Mathematik, Universität Tübingen, Auf der Morgenstelle 10, 72076 Tübingen, Germany
- ³⁾Institute of Physics, NAWI Graz, University of Graz, Universitätsplatz 5, A-8010 Graz, Austria
- ⁴⁾ Particle Physics, Faculty of Physics, University of Vienna, Boltzmanngasse 5, A-1090 Wien, Austria
- ⁵⁾Department of Astronomy and Theoretical Physics, Lund University, Box 43, 221 00 Lund, Sweden

(Dated: 29 September 2022)

We study a class of SU(N) Wigner 6j symbols involving two fundamental representations, and derive explicit formulae for all 6j symbols in this class. Our formulae express the 6j symbols in terms of the dimensions of the involved representations, and they are thereby functions of N. We view these explicit formulae as a first step towards efficiently decomposing SU(N) color structures in terms of group invariants.

I. INTRODUCTION

A unique feature of the characteristic quantum numbers of the strong force as described by Quantum Chromodynamics (QCD) is that they are confined and not observable. In order to extract observable quantities from QCD scattering amplitudes one has to average over external color quantum numbers or, otherwise, project onto definite hadronic states. In both cases the color quantum numbers enter calculations on a similar footing as internal interfering quantum mechanical degrees of freedom. This allows for the usage of color bases which leave out information on the states within an irreducible representation (irrep) of SU(3).

Despite this simplification, one of the challenges in multi-parton QCD calculations is the accurate description of the large color space. Often color-summed/-averaged so-called trace¹⁻¹¹ and color-flow bases¹²⁻¹⁸ are used. These bases take advantage of the possibility to ignore the internal structure of SU(3) irreps, but they also ignore the irreps altogether, i.e. the basis vectors are in no correspondence to the intermediate states in which a set of partons transforms. Moreover, for a finite number N of colors, trace and color-flow bases are non-orthogonal and overcomplete, i.e., strictly speaking, they are not even bases but only spanning sets. The size of theses spanning sets grows roughly as a factorial in the number $n_{g+q\bar{q}}$ of gluons and $q\bar{q}$ -pairs¹⁹. Since these spanning sets are non-orthogonal, this translates, in the worst case, to a factorial square scaling, $(n_{g+q\bar{q}}!)^2$, for the number of inner products that have to be calculated. In a full color description of a scattering cross section this growth will be prohibitive if one calculates all contributing terms and cannot use additional information about the amplitudes or exploit Monte Carlo methods to sample over color structures, as e,q, done in 17 .

An ideal basis would be both orthogonal and minimal, allowing for the smallest number of terms needed when expanding amplitudes and correlation functions in color structures. These properties are combined in multiplet bases^{19–30}, which use representation theory to iteratively group partons into orthogonal states. So far, the use of multiplet bases has been rather limited, in part likely due to the lack of explicit bases for many partons, i.e. the situation in which they would really be advantageous.

In this paper we suggest taking the usage of representation theory one step further: Instead of *explicitly* created bases, we advocate using Wigner 6j coefficients (or 6j symbols or just 6js – we use all these terms interchangeably in this paper) for calculations in color space. This, however, assumes that the required 6j coefficients have been calculated and are readily available also for a high number of partons. In Refs. 25,30 explicit bases were used to calculate 6js for a limited number of partons. This allows for a fast decomposition at use-time, i.e. when the 6js (corresponding to the same bases) are used in actual computations of amplitudes, but the factorial growth of the spanning set remains a challenge at construction time, thereby effectively limiting the number of involved particles to one or a few handfuls.

When decomposing color structures into multiplet bases using 6js, no explicit bases are needed; i.e. all calculations are performed in terms of SU(N) group invariant 6j coefficients, along with dimensions of representations and Wigner 3j coefficients (or 3j symbol, or 3j for short), which may be normalized to 1. This poses the question if it should not also be possible to derive these invariants in terms of themselves. More precisely: Can one derive a consistent set of 6j coefficients only in terms of group invariants, specifically the dimensions of representations?

In this paper we answer this question affirmatively when at least two of the irreps involved in a 6j symbol are fundamental representations, i.e. quark-lines, that do not share a common vertex. In Theorem 1 we present explicit formulae for the absolute values of all 6j symbols in this class. We also explain how to iteratively fix and determine the signs of these 6js, and for $N \leq 3$ we prove (whereas for N > 3 we conjecture) that this procedure always leads to a consistent set of signs. In particular, we have thus determined these 6j symbols in the phenomenologically relevant case N = 3. For N = 2 the problem was generally solved before, see e.g. Ref. 31. In future work we will show how to determine the other 6js required for a full color decomposition. We note that other approaches for calculating SU(3) 6js in terms of Clebsch-Gordan coefficients exist^{32,33}, but stress that our method exploits group invariants only.

We view our results as a first step towards a complete reduction of color space in terms of SU(N) group invariants, which has the potential to significantly simplify fixed-order as well as all-order calculations in color space, ranging from analytic approaches up to Monte Carlo methods. The reduction of color space in terms of invariants also has the potential to provide further insight into other aspects such as the color structure of hadronization models^{34,35}.

This paper is organized as follows: Section II gives a brief introduction to the birdtrack

method for SU(N), illustrating how 6j symbols appear and how they can be used to decompose more general color structures. In Section III we introduce the particular class of 6j symbols of interest to the present paper, and in Section IV we describe properties of general 6j symbols, as well as of the class of symbols studied here. Section V constitutes the main part of this paper, wherein the closed form expressions of the 6js are presented in Theorem 1. The relevance of these results, as well as future work complementing them, are discussed in Section VI.

II. BIRDTRACK METHODS FOR SU(N) COLOR SPACE

In this section we briefly outline how to utilize the birdtrack method for decomposing group invariant (color) structures in terms of dimensions, Wigner-3*j* and Wigner-6*j* symbols. For a full, comprehensive introduction to the birdtrack formalism, readers are referred to Ref. 36. The hasty reader finds a minimal introduction in Appendix A of Ref. 19, whereas a more pedagogical account can be found in Ref. 37. Examples of birdtrack calculations for QCD can be found in Ref. 24,25.

We start out with a reminder that implicit indices of states within a representation are always summed over. We therefore have, for an irrep α ,

i.e. the sum of states within an irrep adds up to the dimension d_{α} of that irrep.

The second simplest color structure that may be encountered, which also contains a sum, is the "self energy" diagram

$$\frac{\alpha}{\delta} = \frac{\alpha}{\alpha} = \frac{\alpha}{\alpha} = \frac{\alpha}{\alpha} \qquad (2)$$

where the free line is to be understood as a Kronecker delta in the representation indices α and β , and the normalization constant can be found by contracting indices on both sides;

as a consistency check, we have

$$\frac{\alpha}{\delta} = \frac{\beta = \alpha}{\delta} = \frac{\alpha}{d_{\alpha}} d_{\alpha} = \frac{\alpha}{\delta} , \qquad (3)$$

where we used Equation (1). The result on the right hand side is known as a 3j symbol. It is proportional to the magnitude of the vertex, and, depending on the vertex normalization, it may thus assume different values. We will keep the normalization of the 3j symbol arbitrary for most of our derivations, although our final results are stated in the normalization where all 3js are normalized to 1. This is in contrast to the standard QCD normalization for which, for example $00000 = \frac{1}{2}(N^2 - 1)$, for the generator normalization $\text{tr}[t^a t^b] = \frac{1}{2}\delta^{ab}$.

After the self-energy, with the topology of a loop involving two internal representations, the next structure to consider is the vertex correction. Here, we also encounter the Wigner-6j symbols for the first time, as they act as normalization constants when eliminating loops with three internal lines,

$$\frac{\beta}{\delta} = \sum_{a} \frac{1}{\alpha} \underbrace{\frac{1}{\alpha}}_{\text{Wigner-6}j} \underbrace{\frac{1}{\alpha}}_{\text{Wigner-6}j}, \qquad (4)$$

where the sum over all possible vertices a collapses to only one term if the irreps α , σ and ρ admit only one vertex. For the particular 6j symbols discussed in this paper, this is always the case. The triangular pictogram in Equation (4) describes a Wigner-6j symbol which, in the case of SU(2), is usually denoted in 2-line notation as

$$\begin{array}{cccc}
\sigma & & & & \\
 & & & \\
 & & \\
 & & \\
 & & \\
 & & \\
 & & \\
 & & \\
 & & \\
 & & \\
 & & \\
 & & \\
 & & \\
 & & \\
 & & \\
 & & \\
 & & \\
 & & \\
 & & \\
 & & \\
 & & \\
 & & \\
 & & \\
 & & \\
 & & \\
 & & \\
 & & \\
 & & \\
 & & \\
 & & \\
 & & \\
 & & \\
 & & \\
 & & \\
 & & \\
 & & \\
 & & \\
 & & \\
 & & \\
 & & \\
 & & \\
 & & \\
 & & \\
 & & \\
 & & \\
 & & \\
 & & \\
 & & \\
 & & \\
 & & \\
 & & \\
 & & \\
 & & \\
 & & \\
 & & \\
 & & \\
 & & \\
 & & \\
 & & \\
 & & \\
 & & \\
 & & \\
 & & \\
 & & \\
 & & \\
 & & \\
 & & \\
 & & \\
 & & \\
 & & \\
 & & \\
 & & \\
 & & \\
 & & \\
 & & \\
 & & \\
 & & \\
 & & \\
 & & \\
 & & \\
 & & \\
 & & \\
 & & \\
 & & \\
 & & \\
 & & \\
 & & \\
 & & \\
 & & \\
 & & \\
 & & \\
 & & \\
 & & \\
 & & \\
 & & \\
 & & \\
 & & \\
 & & \\
 & & \\
 & & \\
 & & \\
 & & \\
 & & \\
 & & \\
 & & \\
 & & \\
 & & \\
 & & \\
 & & \\
 & & \\
 & & \\
 & & \\
 & & \\
 & & \\
 & & \\
 & & \\
 & & \\
 & & \\
 & & \\
 & & \\
 & & \\
 & & \\
 & & \\
 & & \\
 & & \\
 & & \\
 & & \\
 & & \\
 & & \\
 & & \\
 & & \\
 & & \\
 & & \\
 & & \\
 & & \\
 & & \\
 & & \\
 & & \\
 & & \\
 & & \\
 & & \\
 & & \\
 & & \\
 & & \\
 & & \\
 & & \\
 & & \\
 & & \\
 & & \\
 & & \\
 & & \\
 & & \\
 & & \\
 & & \\
 & & \\
 & & \\
 & & \\
 & & \\
 & & \\
 & & \\
 & & \\
 & & \\
 & & \\
 & & \\
 & & \\
 & & \\
 & & \\
 & & \\
 & & \\
 & & \\
 & & \\
 & & \\
 & & \\
 & & \\
 & & \\
 & & \\
 & & \\
 & & \\
 & & \\
 & & \\
 & & \\
 & & \\
 & & \\
 & & \\
 & & \\
 & & \\
 & & \\
 & & \\
 & & \\
 & & \\
 & & \\
 & & \\
 & & \\
 & & \\
 & & \\
 & & \\
 & & \\
 & & \\
 & & \\
 & & \\
 & & \\
 & & \\
 & & \\
 & & \\
 & & \\
 & & \\
 & & \\
 & & \\
 & & \\
 & & \\
 & & \\
 & & \\
 & & \\
 & & \\
 & & \\
 & & \\
 & & \\
 & & \\
 & & \\
 & & \\
 & & \\
 & & \\
 & & \\
 & & \\
 & & \\
 & & \\
 & & \\
 & & \\
 & & \\
 & & \\
 & & \\
 & & \\
 & & \\
 & & \\
 & & \\
 & & \\
 & & \\
 & & \\
 & & \\
 & & \\
 & & \\
 & & \\
 & & \\
 & & \\
 & & \\
 & & \\
 & & \\
 & & \\
 & & \\
 & & \\
 & & \\
 & & \\
 & & \\
 & & \\
 & & \\
 & & \\
 & & \\
 & & \\
 & & \\
 & & \\
 & & \\
 & & \\
 & & \\
 & & \\
 & & \\
 & & \\
 & & \\
 & & \\
 & & \\
 & & \\
 & & \\
 & & \\
 & & \\
 & & \\
 & & \\
 & & \\
 & & \\
 & & \\
 & & \\
 & & \\
 & & \\
 & & \\
 & & \\
 & & \\
 & & \\
 & & \\
 & & \\
 & & \\
 & & \\
 & &$$

For loops with more than three internal representations there is no similar simple expression. Instead, such color structures can be systematically reduced into loops with fewer internal lines by the application of the completeness relation

$$\frac{\beta}{\gamma} = \sum_{\delta} \frac{d_{\delta}}{\beta} \frac{\beta}{\gamma} . \tag{6}$$

Applying this to a loop with more internal irreps, the color structure can be rewritten in terms of a shorter loop and a sum of vertex corrections, which may be removed using Equation (4). Schematically, we have

$$\begin{array}{c|c}
 & \underline{\qquad} & \underline{\qquad$$

which can be fully reduced to 3js, 6js and dimensions by applying the completeness relation two more times. In a similar fashion, loops with yet more internal representations can be reduced back to expressions involving dimensions and 3j and 6j coefficients.

For this reason, to decompose an arbitrary color structure into group invariants, it is in principle enough to know the dimensions which may be calculated using standard methods (see e.g. 36,38,39 , also summarized in Appendix E), the 3j coefficients (which we normalize via the vertices to 1) and the 6j coefficients, a class of which will be derived here.

III. WIGNER-6j SYMBOLS WITH TWO OPPOSING QUARK-LINES

In this work we focus on 6j symbols with (at least) two quark-lines on opposite edges,



where the single lines are understood to be in the fundamental representation, and α , M_i , M_j and M^{ij} are irreps which can be thought about as Young diagrams. For the main part

of this paper, we will assume that none of the irreps labeled by α , M_i , M_j and M^{ij} is the fundamental representation, as this allows us to ignore irrep ordering in vertices (this is explained in detail in Appendix C). However, Appendix D discusses a few special cases where some of these irreps are indeed the fundamental representation corresponding to \square .

The Young diagrams α , M_i , M_j and M^{ij} used in the construction of the 6j symbol given in Equation (8) are related to each other as follows:

- We begin by fixing a Young diagram α .
- Thereafter, we add a single box to α in row i (resp. j) in order to obtain M_i (resp. M_j). Note that, in general, we cannot add a box to every row of α since in some cases the result would not be a Young diagram.
- Lastly, M^{ij} is the diagram obtained from α by adding two boxes, first one in row i and then one in row j. If M_i and M_j both exist, then the final result of adding two boxes is commutative, i.e.

$$\boldsymbol{M}^{ij} = \boldsymbol{M}^{ji} \ . \tag{9}$$

Examples for the construction of M_i , M_j and M^{ij} from a fixed diagram α are given in Figure 1.

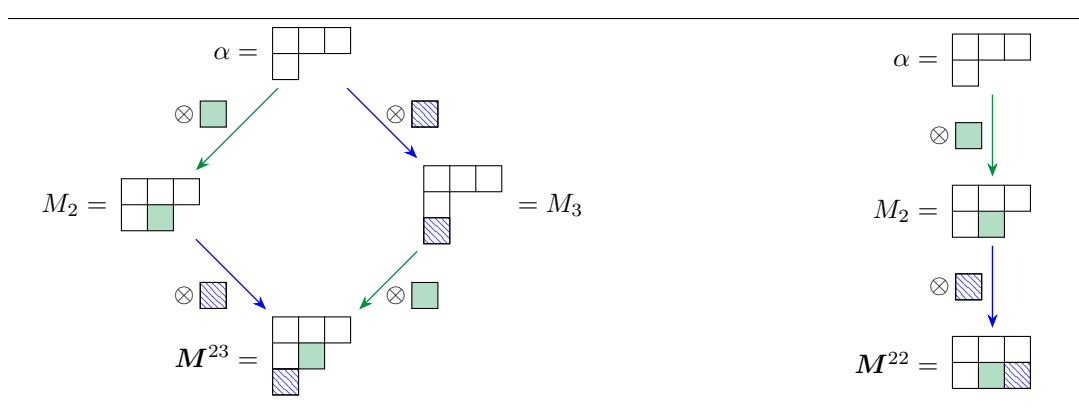
We denote the dimensions of the irreps corresponding to α , M_i , M_j and M^{ij} by d_{α} , d_i , d_j , and d_{ij} , respectively,

$$\dim(\alpha) = d_{\alpha}$$
, $\dim(M_i) = d_i$, $\dim(M_j) = d_j$ and $\dim(\mathbf{M}^{ij}) = d_{ij}$. (10)

These dimensions can be calculated with standard methods from the corresponding diagrams, see Appendix E.

Since the 6j symbols discussed in this paper have the property that the two fundamental lines and the irrep indexed by α are fixed, we may denote the 6j symbol in Equation (8) by $S_{i,j}^{ij}$, where the bottom two indices i, j correspond to the indices of the two diagrams M_i and M_j , and the upper double-index corresponds to the double-index of the diagram M^{ij} ,

$$S_{i,j}^{ij} = M_i \qquad (11)$$



- (a) For i=2 and j=3, we obtain M_2 , M_3 and (b) For i=j=2 we obtain M_2 and M^{22} from M_2 from M_3 from M_4 by adding a green (shaded) box in M_4 and M_4 from M_4 and M_5 from M_4 and M_5 from M_4 and M_5 from M_4 from M_5 and M_5 from M_5 and M_5 from M_5 from M_5 and M_5 from M_5 from M_5 from M_5 and M_5 from M_5 fr
- **FIG. 1:** Two examples constructing M_i , M_j and M^{ij} from the Young diagram $\alpha = \Box$ for different values of i and j.

It should be noted that the irrep M^{ii} (both indices equal), provided it is admissible, is contained in the product $M_j \otimes \square$ if and only if j = i, as is also illustrated in Figure 1b. Thus,

for fixed
$$M^{ii}$$
: $S_{a,b}^{ii} = \delta_{ia}\delta_{ib} \stackrel{M_a}{\longrightarrow}$, (12)

and, similarly,

for fixed
$$M^{ij}$$
: $S_{i,b}^{ij} = \delta_{jb} \stackrel{M_i}{\longrightarrow} .$ (13)

Conversely, if we fix the diagrams M_i and M_j , the only irrep labeled by \mathbf{M}^{ab} that would render the 6j symbol $S_{i,j}^{ab}$ nonzero is precisely that corresponding to \mathbf{M}^{ij} ,

for fixed
$$M_i$$
 and M_j : $S_{i,j}^{ab} = \delta_{ia}\delta_{jb} \stackrel{M_i}{\longrightarrow}$, (14)

and, if i = j,

for fixed
$$M_i$$
 $S_{i,i}^{ab} = \delta_{ia} \stackrel{M_i}{\swarrow}$ (15)

We remark that the 6j symbol in Equation (8) is actually the most general 6j containing two quark-lines not meeting in one vertex: Even though one might suspect that flipping the direction of one or several arrows would lead to further 6j symbols, this is not the case as can be deduced from the discussion in Section IV C. The full set of 6js with two or more quark-lines will, in addition, contain 6js where two quark-lines meet in one vertex. The cases in which both quark-lines are incoming or in which both quark-lines are outgoing in a vertex are discussed in Appendix D. If one of the two quark-lines meeting in a vertex is incoming and the other is outgoing, we have to distinguish two cases: Either the two lines form a singlet (trivial representation), in which case the 6j is reduced to a 3j (up to normalization), or they are in the adjoint representation, i.e. forming a gluon-line. The latter case will be discussed in a future publication, together with other 6j symbols containing gluon-lines. The class of 6js defined by (8) is one that is often encountered in a QCD context, cf. Ref. 30, Equations. (2.7) and (2.8). In future work we will study the remaining 6js needed to decompose color structure, as well as their applications to QCD.

Before we derive relations between 6j symbols of the form (8) in Section V A, we require some more properties of these symbols, which will be discussed in the following Section IV.

IV. PROPERTIES OF 6j SYMBOLS

The present section discusses several properties of 6j symbols that will be used in this paper. First, we briefly discuss irrep line orderings in vertices in Section IV A. Section IV B focuses on symmetries of 6j symbols, where we, in particular, make use of the fact that a 6j symbol in its graphical representation can be viewed as a tetrahedron. In Section IV C we restrict ourselves to the 6j symbols of interest in this paper (i.e. those defined in Section III) and discuss additional symmetries that arise from having two fundamental representations on opposite edges of the 6j.

A. Line ordering in vertices

In birdtrack calculations we may end up with diagrams that are complicated to read because of (unnecessary) line crossings. In such cases it is convenient to introduce barred vertices, indicating that two lines in a vertex have been swapped, i.e. we define

$$\begin{array}{ccc}
\beta & \alpha & \beta & \alpha \\
\gamma & & &
\end{array}
\qquad (16)$$

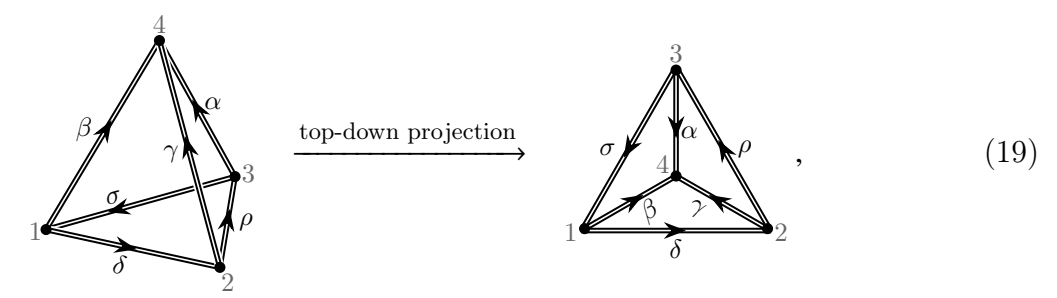
Fortunately, for most vertices appearing in this work, the bars can be omitted again in the next step as we explain in Appendix C. The only vertex relevant for this work for which line swapping leads to a phase change is the vertex that is used for the antisymmetric projection of two quark-lines, for which we have

However, since there are only a few 6j symbols satisfying the conditions laid out in Section III that also contain the vertex in Equation (17), we discuss these separately in Appendix D, and assume for the remainder of this paper that all vertices appearing in the 6j symbols in question are equal to their barred counterparts,

$$\beta \gamma \alpha = \beta \gamma \alpha \qquad \text{if } \alpha \neq \beta \neq \gamma \neq \alpha .$$
(18)

B. Symmetries of general 6 i symbols

A Wigner-6j symbol in its graphical *birdtrack* form may be thought of as a tetrahedron, where our usual notation represents a top-down planar projection. For example, for a 6j symbol connecting general irreps α , β , γ , δ , ρ and σ ,



where we have labeled the vertices of the tetrahedron and the corresponding 6j as 1, 2, 3, 4 for visual clarity. Clearly, which of the four vertices of the tetrahedron we view as the top

vertex is a completely arbitrary choice and thus cannot affect the 6j symbol in any way. Therefore, we find that

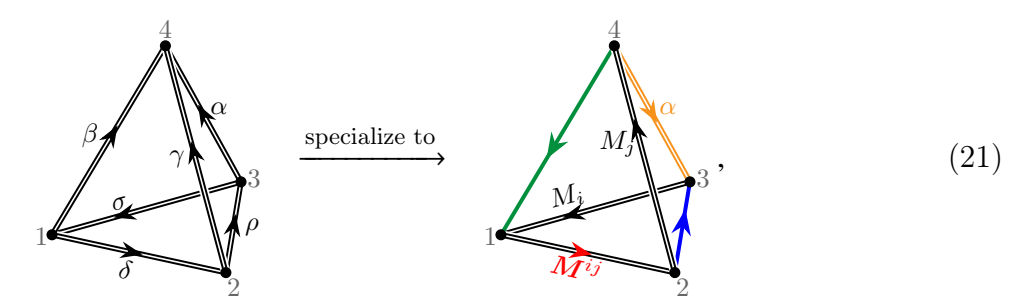
$$\frac{\sigma}{4} \frac{\alpha}{\alpha} \rho = \alpha \frac{4}{100} \gamma = \beta \frac{4}{200} \alpha = \gamma \frac{4}{300} \beta . \quad (20a)$$

By that same token, a rotation by 60° also leaves the 6j symbol unchanged,

$$\frac{\sigma}{\delta} = \frac{\rho}{\delta} = \frac{\rho}{\delta} = \frac{\delta}{\delta} = \frac{\delta$$

C. Symmetry properties of 6j symbols with two quark-lines

In the present paper, we want to focus on 6j symbols that were described in Section III,

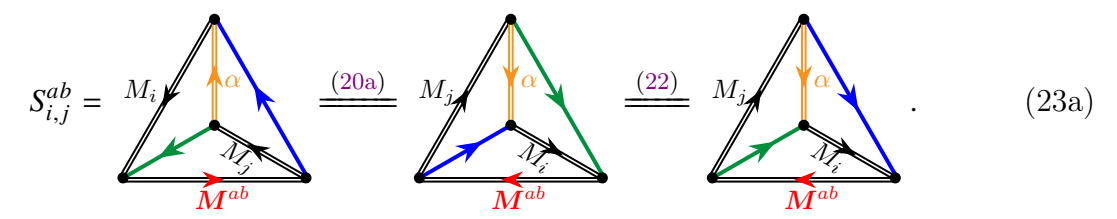


which affords us additional symmetries. Firstly, since the two quark-lines (the blue and green single lines) are both in the fundamental representation, we may "exchange" them without changing the 6j symbol,

we will, however, continue to draw the two quark-lines in different colors for visual clarity, as this will make the discussions that follow (in particular those of Appendix A) more legible.

Consider $S_{i,j}^{ab}$ corresponding to the last expression in Equation (20a) and exchange the green and blue fundamental lines according to Equation (22) to end up with the following

graphical form of $S_{i,j}^{ab}$,



If we form the complex conjugate of this depiction of the 6j symbol (which, in the birdtrack formalism, is done by reversing all arrows and barring all vertices, cf. Appendix C), we will obtain a different 6j symbol, namely $S_{j,i}^{ab}$ (notice the order of the lower indices),

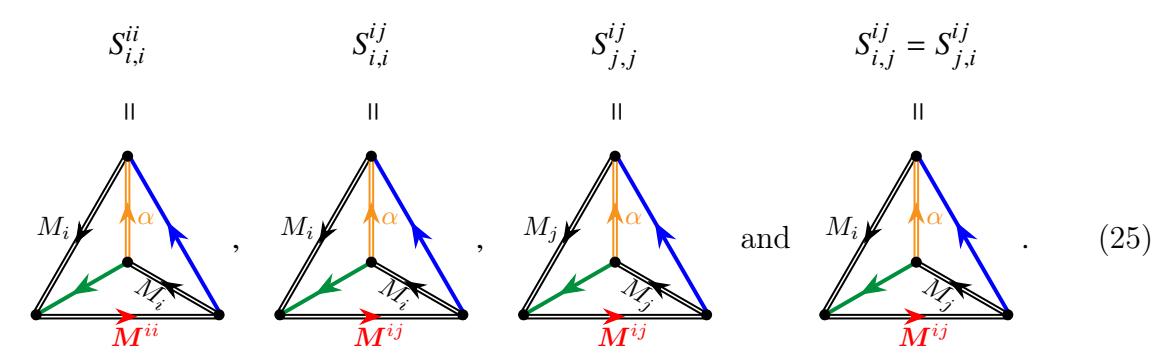
$$(S_{i,j}^{ab})^* = \begin{pmatrix} M_j & & \\ & &$$

where we were able to ignore the bars on the vertices in the middle 6j symbol as we assume that all of its vertices obey Equation (18). (All 6j symbols encountered here, not satisfying this, are the ones involving (17). These are discussed separately in Appendix D).

It is easy to convince oneself that all 6js naturally can be chosen to be real by writing out representations in terms of the fundamental representations and symmetrizers and anti-symmetrizers. Contracting all quark-lines yields a real polynomial in N, such that $S_{i,j}^{ab} \in \mathbb{R}$, and it follows that $(S_{i,j}^{ab})^* = S_{i,j}^{ab}$, and hence

$$S_{i,j}^{ab} = S_{j,i}^{ab} . (24)$$

In conclusion, for fixed i, j with $i \neq j$, there are four distinct types of 6j symbols, namely



In the following Section V we proceed to first derive relations between these four 6j symbols, and then solve this system of equations to obtain their closed form expressions.

V. CLOSED FORM EXPRESSIONS OF 6j SYMBOLS

In the present section, we present several relations between the four 6j symbols given in Equation (25). In Section VB, we use these relations to find closed form expressions of the 6j symbols. These expressions are summarized in Theorem 1, which is the main result of this paper.

A. Relations between 6j symbols

Through the repeated use of the completeness relation Equation (6) and the vertex correction Equation (4), we find the following relations between the four distinct 6j symbols given in Equation (25) (the derivations can be found in Appendix A):

1. For a given representation M^{ij} , we obtain

$$1 = (d_i)^2 (S_{ij}^{ij})^2 + d_i d_j (S_{ij}^{ij})^2 . (26a)$$

Furthermore,

$$0 = d_i S_{i,i}^{ij} S_{i,j}^{ij} + d_j S_{i,j}^{ij} S_{i,j}^{ij} . {26b}$$

2. For two given representations M_i and M_j , we obtain

$$\frac{1}{d_{\alpha}} = \sum_{Mab} d_{ab} (S_{i,j}^{ab})^2 , \qquad (26c)$$

where d_{ab} is the dimension of the representation M^{ab} .

3. For a given representation M_i , we have

$$1 = \sum_{b} d_{ib} S_{i,i}^{ib} . \tag{26d}$$

Notice that, in these relations, all 3j symbols were set to 1; the derivations in Appendix A keep all 3js explicit until the very last step.

B. Solving for closed form expressions

In the present section, we derive closed form expressions for the 6j symbols using the relations presented in the previous Section V A. For the purpose of this section, we assume

that all the 6js appearing in these relations are admissible (that is boxes can be added in rows i and j for the particular diagram α from which we start).

Let us start with Equation (26a): Notice that, if we choose the representation M^{ij} such that i = j, $M^{ij} \to M^{ii}$, the second term vanishes in accordance with Equation (12), such that Equation (26a) reduces to

Equation (26a)
$$\xrightarrow{M^{ij} \to M^{ii}} 1 = (d_i)^2 (S_{i,i}^{ii})^2$$

$$\iff S_{i,i}^{ii} = \pm \frac{1}{d_i} . \tag{27}$$

In fact, in Appendix B 1 we show that this 6j symbol is always positive, such that

$$S_{i,i}^{ii} = \frac{1}{d_i} (28)$$

If in Equation (26c) we instead choose $i \neq j$ (i.e. we choose M_i and M_j to be inequivalent), there is only one possible M^{ab} that renders the 6j nonzero, namely M^{ij} (this follows from condition (14)). Thus, the sum on the right hand side of Equation (26c) reduces to one term, allowing us to solve for yet another 6j symbol,

Equation (26c)
$$\xrightarrow{i\neq j}$$
 $\frac{1}{d_{\alpha}} = d_{ij} (S_{i,j}^{ij})^2$ $\iff S_{i,j}^{ij} = \pm \frac{1}{\sqrt{d_{\alpha}d_{ij}}}$ (29)

In Appendix B 2 we explain how the overall sign of $S_{i,j}^{ij}$ can be chosen.

We may now plug the result for $S_{i,j}^{ij}$ back into the full form of Equation (26a) to also obtain a closed form expression for $S_{i,j}^{ij}$,

$$1 = (d_{i})^{2} (S_{i,i}^{ij})^{2} + d_{i}d_{j} (S_{i,j}^{ij})^{2} \xrightarrow{(S_{i,j}^{ij})^{2} = \frac{1}{d_{\alpha}d_{ij}}}} 1 = (d_{i})^{2} (S_{i,i}^{ij})^{2} + \frac{d_{i}d_{j}}{d_{\alpha}d_{ij}}$$

$$\iff S_{i,i}^{ij} = \pm \frac{1}{d_{i}} \sqrt{1 - \frac{d_{i}d_{j}}{d_{\alpha}d_{ij}}}. \tag{30}$$

Lastly, since by Equation (29) $S_{i,j}^{ij} \neq 0$, we may now derive the last 6j symbol, namely $S_{j,j}^{ij}$, using relation (26b):

$$0 = d_{i}S_{i,i}^{ij}S_{i,j}^{ij} + d_{j}S_{j,j}^{ij}S_{i,j}^{ij} = (d_{i}S_{i,i}^{ij} + d_{j}S_{j,j}^{ij})S_{i,j}^{ij}$$

$$\xrightarrow{S_{i,j}^{ij} \neq 0} d_{j}S_{j,j}^{ij} = -d_{i}S_{i,i}^{ij} = \mp \sqrt{1 - \frac{d_{i}d_{j}}{d_{\alpha}d_{ij}}}.$$
(31)

In Appendix B 3 we show how the signs of $S_{i,i}^{ij}$ (and hence $S_{j,j}^{ij}$) can be uniquely determined from Equation (26d) for $N \leq 3$.

In summary:

Theorem 1 (Closed form expressions for the distinct 6j symbols) For each of the distinct 6j symbols identified in Equation (25), we obtain the following closed form expression:

$$S_{i,i}^{ii} = \frac{1}{d_i} \quad , \qquad d_i S_{i,i}^{ij} = \pm \sqrt{1 - \frac{d_i d_j}{d_\alpha d_{ij}}} = -d_j S_{j,j}^{ij} \quad , \qquad S_{i,j}^{ij} = \pm \frac{1}{\sqrt{d_\alpha d_{ij}}} \quad , \tag{32}$$

where the sign of the $S_{i,j}^{ij}$ depends on the definition of the vertices as discussed in Appendix B2. The signs of $S_{i,i}^{ij}$ (equivalently $S_{j,j}^{ij}$) can be uniquely determined from Equation (26d) for $N \leq 3$, cf. Appendix B3.

We remark that, with the above, the problem of calculating Wigner-6j symbols with quark-lines on opposing edges has been reduced to finding the dimensions of the representations. Once these are known, given that a starting representation α results in a maximal number of new 6j symbols, the scaling of finding all relevant 6js (of the given form) with n boxes is therefore given by the number of possible representations α with n-2 boxes, which scales as n for N=3. This implies that finding all 6js with n0 boxes scales only as n2 for n3.

VI. CONCLUSIONS AND OUTLOOK

In this paper we have taken the first steps towards deriving Wigner 6j coefficients in terms of SU(N) group invariants only by writing down closed form expressions of a set of 6js involving at least two fundamental representations.

We are presently supplementing this with a limited set of 6js involving the adjoint representation, which will be enough to allow for a complete color decomposition of amplitudes in QCD³⁰. While the 6js with two quark-lines are expressed in terms of dimensions only, the gluon 6js require the quark 6js. Beyond this one may anticipate that yet more general 6js would be similarly expressible.

Once complemented with the gluon 6js, we expect these sets of 6js to have significant phenomenological relevance by opening up, for the first time, the possibility to work with orthogonal physical states also for processes involving many partons.

ACKNOWLEDGMENTS

MS acknowledges support by the Swedish Research Council (contract number 2016-05996, as well as the European Union's Horizon 2020 research and innovation programme (grant agreement No 668679). MS and SP have in part also been supported by the European Union's Horizon 2020 research and innovation programme as part of the Marie Sklodowska-Curie Innovative Training Network MCnetITN3 (grant agreement no. 722104). JAZ is thankful to the Alexander von Humboldt Foundation for support via the Fellowship for Postdoctoral Researchers, as well as to the Erwin Schrödinger Institute for their support via the Junior Research Fellowship. This stay at ESI was essential for the completion of this work. We are also grateful to the Erwin Schrödinger Institute Vienna for hospitality and support while significant parts of this work have been started within the Research in Teams programme "Amplitude Level Evolution II: Cracking down on color bases" (RIT0521).

Appendix A: Relating different 6j symbols

In this appendix, we derive Equations (26a) to (26d), which were used to obtain the closed form expressions of the 6j symbols given in Theorem 1. These derivations make extensive use of the birdtrack formalism introduced in Section II.

1. Proof of Equations (26a) and (26b)

Let α be a particular Young diagram, and let M_i and M^{ij} be obtained from α in accordance with Section III. Then, we may consider the following birdtrack diagram,

$$\begin{array}{cccc}
& & & \\
& & & \\
& & & \\
& & & \\
& & & \\
& & & \\
& & & \\
& & & \\
& & & \\
& & & \\
& & & \\
& & & \\
& & & \\
& & & \\
& & & \\
& & & \\
& & & \\
& & & \\
& & & \\
& & & \\
& & & \\
& & & \\
& & & \\
& & & \\
& & & \\
& & & \\
& & & \\
& & & \\
& & & \\
& & & \\
& & & \\
& & & \\
& & & \\
& & & \\
& & & \\
& & & \\
& & & \\
& & & \\
& & & \\
& & & \\
& & & \\
& & & \\
& & & \\
& & & \\
& & & \\
& & & \\
& & & \\
& & & \\
& & & \\
& & & \\
& & & \\
& & & \\
& & & \\
& & & \\
& & & \\
& & & \\
& & & \\
& & & \\
& & & \\
& & & \\
& & & \\
& & & \\
& & & \\
& & & \\
& & & \\
& & & \\
& & & \\
& & & \\
& & & \\
& & & \\
& & & \\
& & & \\
& & & \\
& & & \\
& & & \\
& & & \\
& & & \\
& & & \\
& & & \\
& & & \\
& & & \\
& & & \\
& & & \\
& & & \\
& & & \\
& & & \\
& & & \\
& & & \\
& & & \\
& & & \\
& & & \\
& & & \\
& & & \\
& & & \\
& & & \\
& & & \\
& & & \\
& & & \\
& & & \\
& & & \\
& & & \\
& & & \\
& & & \\
& & & \\
& & & \\
& & & \\
& & & \\
& & & \\
& & & \\
& & & \\
& & & \\
& & & \\
& & & \\
& & & \\
& & & \\
& & & \\
& & & \\
& & & \\
& & & \\
& & & \\
& & & \\
& & & \\
& & & \\
& & & \\
& & & \\
& & & \\
& & & \\
& & & \\
& & & \\
& & & \\
& & & \\
& & & \\
& & & \\
& & & \\
& & & \\
& & & \\
& & & \\
& & & \\
& & & \\
& & & \\
& & & \\
& & & \\
& & & \\
& & & \\
& & & \\
& & & \\
& & & \\
& & & \\
& & & \\
& & & \\
& & & \\
& & & \\
& & & \\
& & & \\
& & & \\
& & & \\
& & & \\
& & & \\
& & & \\
& & & \\
& & & \\
& & & \\
& & & \\
& & & \\
& & & \\
& & & \\
& & & \\
& & & \\
& & & \\
& & & \\
& & & \\
& & & \\
& & & \\
& & & \\
& & & \\
& & & \\
& & & \\
& & & \\
& & & \\
& & & \\
& & & \\
& & & \\
& & & \\
& & & \\
& & & \\
& & & \\
& & & \\
& & & \\
& & & \\
& & & \\
& & & \\
& & & \\
& & & \\
& & & \\
& & & \\
& & & \\
& & & \\
& & & \\
& & & \\
& & & \\
& & & \\
& & & \\
& & & \\
& & & \\
& & & \\
& & & \\
& & & \\
& & & \\
& & & \\
& & & \\
& & & \\
& & & \\
& & & \\
& & & \\
& & & \\
& & & \\
& & & \\
& & & \\
& & & \\
& & & \\
& & & \\
& & & \\
& & & \\
& & & \\
& & & \\
& & & \\
& & & \\
& & & \\
& & & \\
& & & \\
& & & \\
& & & \\
& & & \\
& & & \\
& & & \\
& & & \\
& & & \\
& & & \\
& & & \\
& & & \\
& & & \\
& & & \\
& & & \\
& & & \\
& & & \\
& & & \\
& & & \\
& & & \\
& & & \\
& & & \\
& & & \\
& & & \\
& & & \\
& & & \\
& &$$

We may insert a completeness relation (cf. Equation (6)) between α and the green (top) quark-line to obtain,

$$\frac{\partial}{\partial a} M_i M^{ij} = \sum_b \frac{d_b}{\partial a} \frac{\partial}{\partial a} M_b M^{ij}; \qquad (A2)$$

from this it is clear that the diagrams M_b are also obtained from α by adding a single box (corresponding to the top quark-line).

The vertex correction on the right-hand side of Equation (A2) gives rise to a 6j symbol (cf. Equation (4)),

$$\frac{1}{M_b} \frac{1}{\alpha M_i} \frac{1}{M^{ij}} = \frac{1}{M_b} \frac{1}{M^{ij}}, \quad (A3)$$

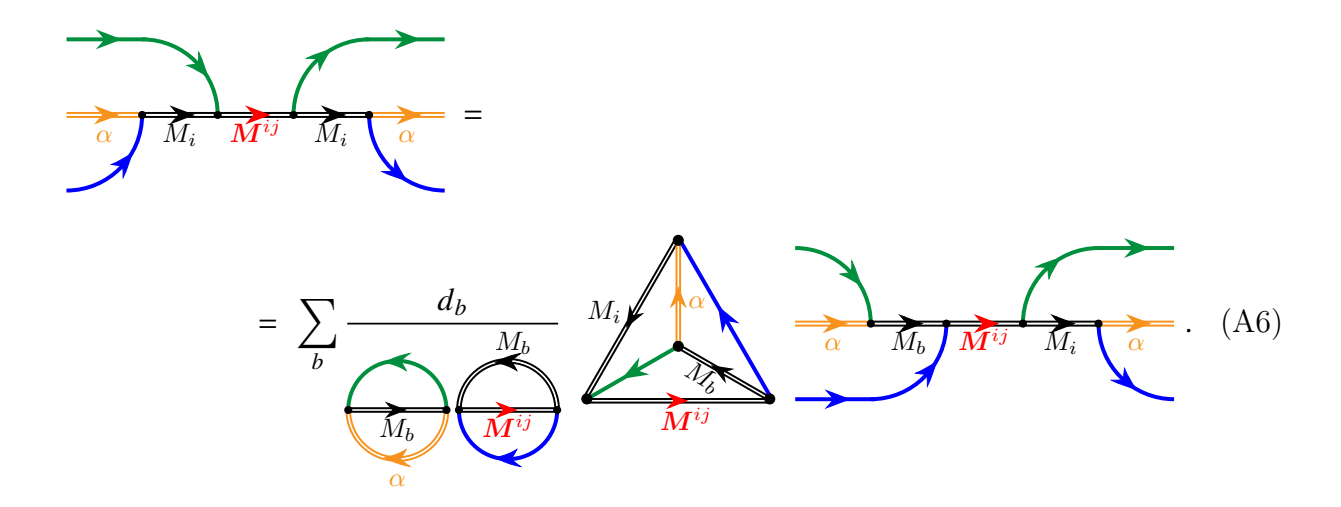
and allows us to rewrite Equation (A2) as

$$\frac{\partial}{\partial a} M_i M^{ij} = \sum_b \frac{d_b}{M_b} M_i M^{ij} . \tag{A4}$$

a. Proof of Equation (26a): Consider the Hermitian conjugate of the expression in Equation (A1) (formed by flipping the birdtrack about the vertical axis and reversing all arrows, cf. Ref. 36),

$$\begin{pmatrix} & & & \\ & & & \\ & & & \\ & & & \\ & & & \\ & & & \\ & & & \\ & & & \\ & & & \\ & & \\ & & & \\$$

and multiply it from the right onto Equation (A4),



Let us now take the trace of this equation: the left-hand side yields a product of 3j symbols,

$$= \frac{M_i}{d_i}, \qquad (A7)$$

while the trace of the birdtrack on the right-hand side gives us yet another 6j symbol,

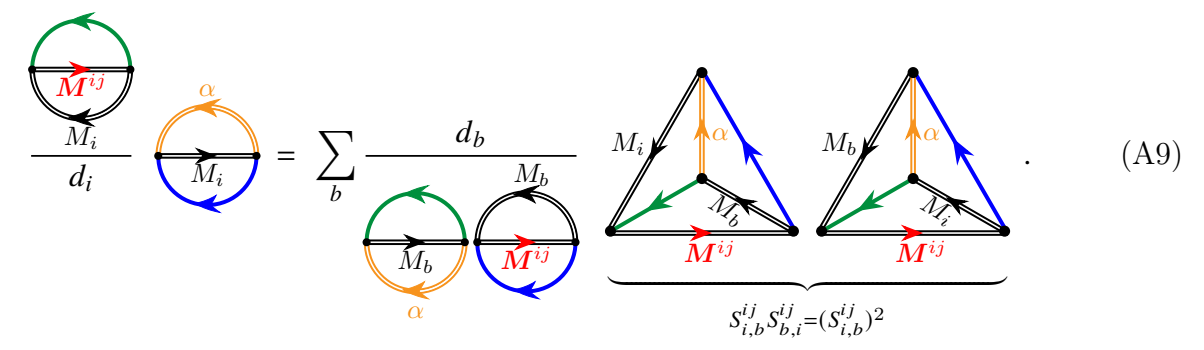
$$= M_b \qquad = M_b \qquad ; \qquad (A8)$$

$$M^{ij} \qquad M_i \qquad ; \qquad M^{ij}$$

we were able to ignore the bars on all vertices as we assume that all representations meeting in any particular vertex are distinct, cf. Equation (18) (special cases not obeying this property are discussed separately in Appendix D).

Putting all of these pieces together, the trace of Equation (A6) amounts to the following

expression,



Since we are allowed to set all the 3j symbols simultaneously to 1, this reduces to

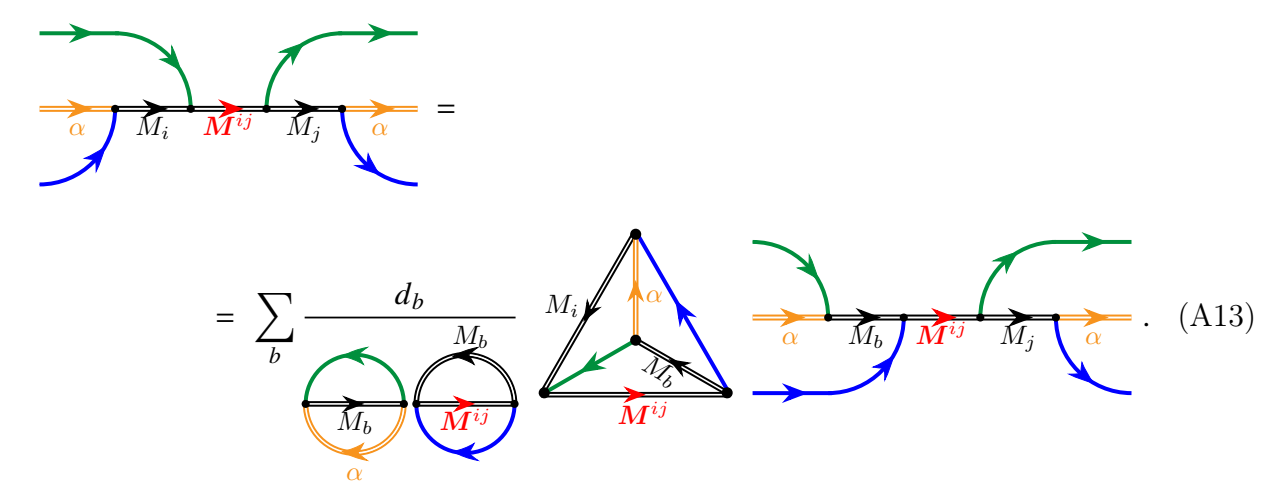
$$1 = d_i \sum_b d_b (S_{ib}^{ij})^2 . (A10)$$

Now, since M^{ij} is fixed, the only way for the 6j symbol $S^{ij}_{i,b}$ to be nonzero is if $b \in \{i, j\}$ (cf. Equation (13)). Hence, the sum on the right-hand side in Equation (A10) only has two terms, leaving us with the desired relation (26a),

$$1 = (d_i)^2 (S_{i,i}^{ij})^2 + d_i d_j (S_{i,j}^{ij})^2 . (A11)$$

b. Proof of Equation (26b): In an analogous way in which we built up the diagram in Equation (A1), let us now consider the diagram

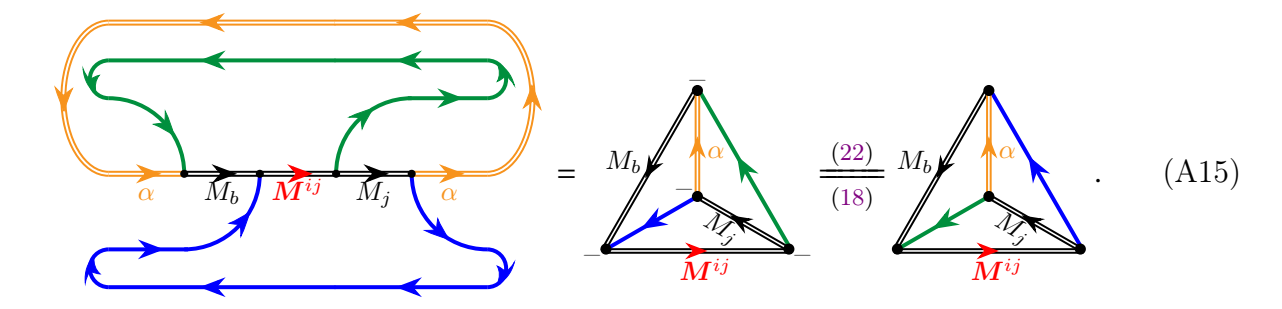
such that $i \neq j$ — in other words M_i and M_j label inequivalent irreps. Similarly to what we did in Equation (A6), let us take the Hermitian conjugate of (A12) and multiply it onto Equation (A4) from the right-hand side,



Again, we will take the trace of this equation: Since $i \neq j$ (that is M_i and M_j label inequivalent irreps), the left-hand side vanishes,

$$\alpha = 0. (A14)$$

The trace of the birdtrack on the right-hand side once again gives us a 6j symbol,



Putting all of the pieces together, we obtain the following relation,

$$0 = \sum_{b} \frac{d_{b}}{M_{b}} M_{ij} M_{ij}$$

$$= S_{i,b}^{ij} S_{b,j}^{ij}$$

$$(A16)$$

We will again set the 3j symbols to 1 such that this equation becomes

$$0 = \sum_{b} d_b S_{i,b}^{ij} S_{b,j}^{ij} . (A17)$$

Recalling that, since M^{ij} is fixed, the only way for the 6j symbols to be nonzero is if $b \in \{i, j\}$ in accordance with Equation (13). Therefore, the sum in Equation (A17) again only has two terms, leaving us with the desired result,

$$0 = d_i S_{i,i}^{ij} S_{i,j}^{ij} + d_j S_{i,j}^{ij} S_{j,j}^{ij} . (A18)$$

2. Proof of Equation (26c)

Let α be a particular Young diagram and let M_i and M_j be obtained from α by adding a box to row i and j, respectively (in accordance with Section III). Then, we may consider the following birdtrack diagram,

We may now insert a completeness relation between M_i and the green (top) quark-line to obtain

$$\frac{\alpha}{\alpha} M_i \alpha M_j \alpha = \sum_{M^{ab}} \frac{d_{ab}}{M_i} \alpha M_i \alpha M_j \alpha . \tag{A20}$$

On the right hand side of this equation we obtain a 6j symbol from the vertex correction,

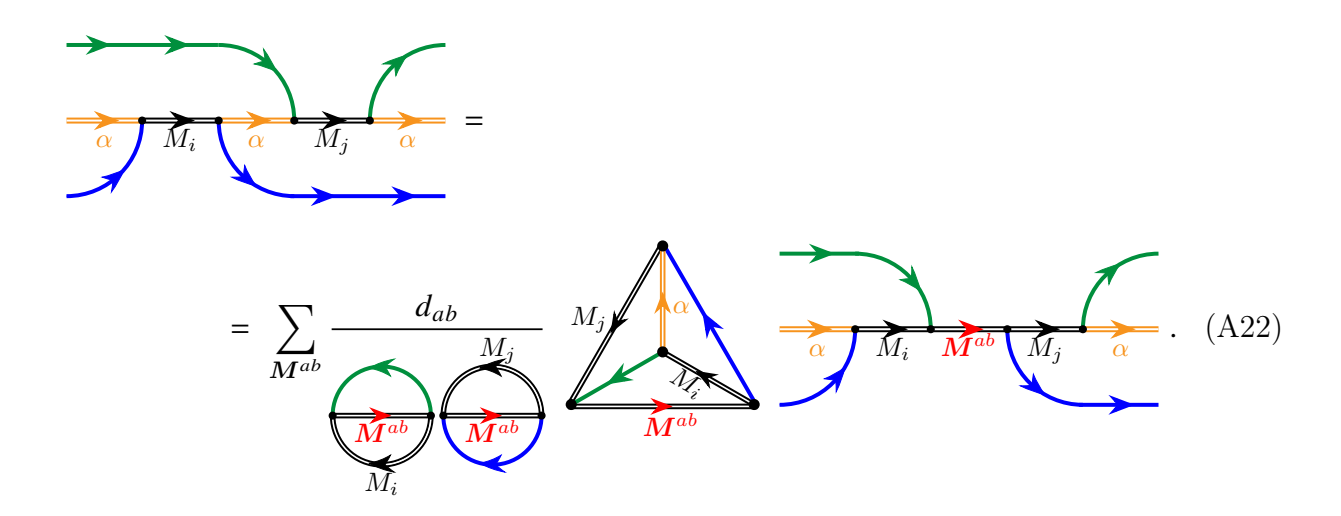
$$\frac{1}{M^{ab}} M_{i} \alpha M_{j} = \frac{1}{M^{ab}} M_{i} M_{j}$$

$$\frac{(22)}{(18)} \frac{1}{M^{ab}} M_{j}$$

$$\frac{M^{ab}}{M^{ab}} M_{j}$$

$$M^{ab} M_{j}$$

such that Equation (A20) reduces to



Let us now take the trace of Equation (A22): When tracing the birdtrack diagram on the left-hand side, we simply get a product of 3j symbols with a dimension factor,

$$= \frac{\alpha}{d_{\alpha}} M_{i} \qquad (A23)$$

The trace of the birdtrack on the right-hand side of Equation (A22) yields another 6j symbol,

$$\alpha = M_i \qquad (A24)$$

$$M^{ab} \qquad M_j \qquad \alpha$$

Substituting expressions (A23) and (A24) back into the traced Equation (A22) yields

$$\frac{\alpha}{d_{\alpha}} = \sum_{\mathbf{M}^{ab}} \frac{d_{ab}}{\mathbf{M}^{ab}} \underbrace{M^{ab}}_{\mathbf{M}^{ab}} \underbrace{M^{ab}}_{\mathbf{M}^{ab}} \underbrace{M^{ab}}_{\mathbf{M}^{ab}}, \quad (A25)$$

where we used Equation (24) to write $S_{j,i}^{ab}S_{i,j}^{ab} = (S_{i,j}^{ab})^2$ (6js for which this relation does not hold are discussed separately in Appendix D). We once again use the fact that we may set all the 3j symbols simultaneously to 1 to finally obtain the desired Equation (26c),

$$\frac{1}{d_{\alpha}} = \sum_{M^{ab}} d_{ab} (S_{i,j}^{ab})^2 , \qquad (A26)$$

again with the only exception of 6j-symbols involving the antisymmetric vertex in eq. (17).

3. Proof of the linear relation Equation (26d)

Let M_i be a particular Young diagram obtained from α by adding a single box, and consider the following birdtrack diagram

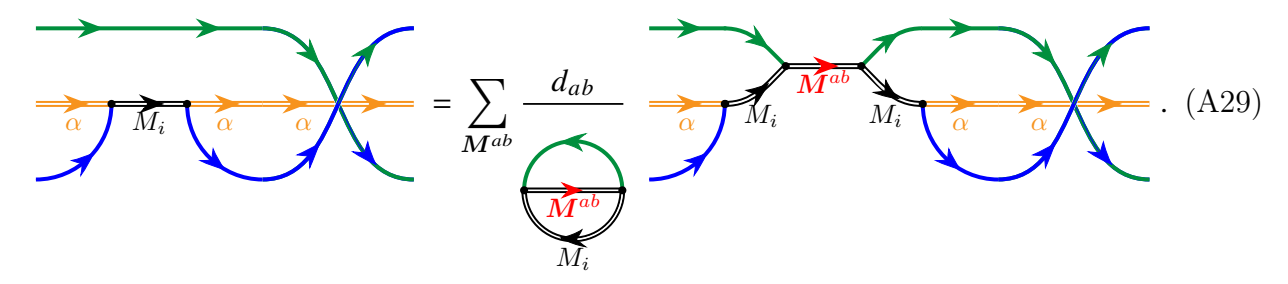
$$(A27)$$

Let us now insert a completeness relation (cf. Equation (6)) between M_i and the green (top) quark-line,

$$\frac{\partial}{\partial a} M_i = \sum_{\mathbf{M}^{ab}} \frac{d_{ab}}{\mathbf{M}^{ab}} \qquad (A28)$$

If we were to take a trace of this equation, we would obtain a bunch of 3j symbols, which is not particularly interesting. However, instead of merely taking a trace, let us first "swap"

the two quark-lines (i.e. we multiply Equation (A28) with a transposition between the two quark-lines from the right). This is a perfectly legal thing to do as the two quark-lines are both in the fundamental representation by definition,



If we now take the trace of this equation, the left-hand side will still yield a 3j symbol,

$$= \underbrace{M_i}^{\alpha}, \qquad (A30)$$

but the right-hand side yields a 6j symbol,

$$= M_i \qquad \alpha \qquad = S_{ii}^{ab} . \tag{A31}$$

The symbol $S^{ab}_{i,\bar{i}}$ is similar to the 6j symbol $S^{ab}_{i,i}$, except the bar over one of the indices, \bar{i} , indicates that the vertices adjacent to one representation line M_i have been conjugated.

Putting the pieces together, we find that

$$\frac{\alpha}{M_i} = \sum_{\mathbf{M}^{ab}} \frac{d_{ab}}{M_i} \qquad M_i$$

$$\frac{M^{ab}}{S_{i,\bar{i}}^{ab}} \qquad (A32)$$

Once again, we ignore the conjugated vertices on the 6j symbol $S^{ab}_{i,\bar{i}}$ as we assume that Equation (18) holds, and refer the reader to Appendix D for all 6j symbols for which the assumption (18) is not valid. Thus, we have that $S^{ab}_{i,\bar{i}} = S^{ab}_{i,i}$, and Equation (A32) reduces to

$$\frac{\alpha}{M_i} = \sum_{\mathbf{M}^{ab}} \frac{d_{ab}}{M_i} \qquad M_i$$

$$\frac{M^{ab}}{M_{ib}} \qquad (A33)$$

Lastly, setting all 3j symbols to 1, we obtain the desired Equation (26d),

$$1 = \sum_{b} d_{ib} S_{i,i}^{ib} , \qquad (A34)$$

where we used the fact that at least one of the indices a, b (which one doesn't matter due to Equation (9)) must be equal to i for the 6j symbol to be nonzero, cf. Equation (15).

Appendix B: Fixing the sign ambiguity

In this section, we will determine the signs for the 6j symbols $S^{ii}_{i,i}$, $S^{ij}_{i,j}$ and $S^{ij}_{i,i} = -\frac{d_j}{d_i} S^{ij}_{j,j}$ in Appendices B 1 to B 3, respectively. For the first two cases $(S^{ii}_{i,i} \text{ and } S^{ij}_{i,j})$, the overall sign can be determined in an N-independent way. For the last case $(S^{ij}_{i,i} = -\frac{d_j}{d_i} S^{ij}_{j,j})$ we are able to determine the signs uniquely for $N \leq 3$, but argue that further work is needed to reliably determine the signs for N > 3.

1. Fixing the sign of $S_{i,i}^{ii}$

We start by determining the sign of $S_{i,i}^{ii}$: Let us now recall that, by the definition of the 6j symbols given in Section III, i denotes the row of α at the end of which the new box was added. In particular, this means that the two boxes were added to the *same* row for the symbol $S_{i,i}^{ii}$, implying that the two quark-lines enter symmetrically in M^{ii} . Let us now

re-draw the 6j symbol somewhat:

$$S_{i,i}^{ii} = M_i \qquad M_i \qquad M_i \qquad M_i . \tag{B1}$$

$$S_{i,i}^{ii} = M_i \qquad M_i = M_i \qquad M_i \qquad M_i.$$
 (B2)

Since the two quark-lines enter symmetrically in M^{ii} , the last term in Equation (B2) vanishes. More precisely, rewriting the triple product $\alpha \otimes \square \otimes \square$ as $(\alpha \otimes \square) \oplus (\alpha \otimes \square)$ and decomposing the result into irreps, one can check that M^{ii} appears in $\alpha \otimes \square$ but not in $\alpha \otimes \square$. Thus, writing $\square \square = \frac{1}{2} (\square \square + \square \square)$,

$$S_{i,i}^{ii} = M_i \qquad M_i = \frac{1}{2} \left(M_i + M_i \right) \qquad (B3)$$

Recognizing the second term of the right-hand side as $\frac{1}{2}S_{i,i}^{ii}$ and taking it to the left-hand side, we notice that the right-hand side reduces to a product of 3j symbols with a dimension factor,

$$S_{i,i}^{ii} = M_i \qquad M_i = M_i \qquad M_i = M_i \qquad (B4)$$

Again setting the 3j symbols to 1, we obtain that

$$S_{i,i}^{ii} = \frac{1}{d_i} , \qquad (B5)$$

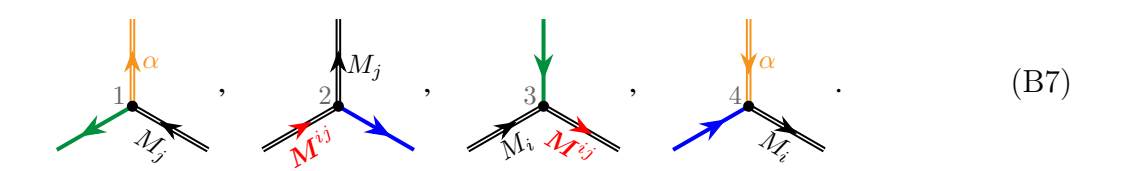
now with a definite sign. We comment that, in determining the sign of $S_{i,i}^{ii}$, we actually rederived $S_{i,i}^{ii}$ with a definite sign. However, since similar methods will not work for $S_{i,j}^{ii}$, $S_{i,j}^{jj}$, and $S_{i,j}^{ij}$, we view this as a consistency check and continue to use Equations (26) to derive the functional forms of the remaining 6j symbols.

2. Fixing the sign of $S_{i,j}^{ij}$ for $i \neq j$

Consider the graphical notation for $S_{i,j}^{ij}$,

$$S_{i,j}^{ij} = \underbrace{M_i}_{1} \underbrace{M_{ij}}_{2}. \tag{B6}$$

Notice that each vertex occurs exactly once in this 6j symbol,



The overall sign of the 6j symbol $S_{i,j}^{ij}$ is uniquely determined by how one decided to define the vertices that occur in this 6j symbol. When iteratively computing these 6j symbols, starting with small Young diagrams and then adding more and more boxes, we may encounter vertices that were already used for earlier 6js. If all four vertices have been encountered earlier then the sign of the 6j symbol may already be fixed. Otherwise we can pick the sign of the 6j to be, say, positive, thus imposing a constraint on signs of the vertices. Often a pair of vertices (either vertices 1 and 4 or vertices 2 and 3) is encountered for the first time in the 6j symbol to compute. Then, picking the sign of the 6j puts a constraint on the product of the signs of the newly encountered vertex pair. Since fully contracted color structures consist of dimensions, 3j symbols and 6j symbols only, the information used and obtained in an iterative computation of 6j symbols is sufficient to perform calculations in color space.

3. Fixing the sign of $S_{i,i}^{ij}$ for $i \neq j$ (equivalently $S_{i,j}^{ij}$)

Lastly, we turn to the 6j symbols $S_{i,i}^{ij}$ and, equivalently, $S_{j,j}^{ij}$, whose functional form is given in Theorem 1. We notice that, for these 6j symbols, each vertex occurs together with its complex conjugated version. Thus, merely the vertex definitions do not determine the overall sign but a different method has to be chosen.

In the present section we will discuss how the linear relation (26d) can be used to fix the signs of $S_{i,i}^{ij}$ and $S_{j,j}^{ij}$ for $N \leq 3$, and comment on why additional work is needed to reliably fix the signs beyond N = 3. However, since our focus lies on physics applications (which will be discussed in a future paper), it is sufficient to fix the signs for N = 3, where N is interpreted as the number of colors N_c .

We require two preliminary results:

Lemma 1 (Determining the relative signs in a sum) Consider the set of known, positive, real numbers $\{A_i\}_{i=1}^k$, and suppose that

$$\sum_{i=1}^{k} \chi_i A_i = C , \qquad (B8)$$

where $C \in \mathbb{R} \setminus \{0\}$ is also known, and the $\chi_i \in \{-1, 1\}$ are to be determined. Then, if all subsets of $\{A_i\}_{i=1}^k$ satisfy

$$\sum_{l=1}^{m \le k} \chi_{j_l} A_{j_l} \neq 0 , \qquad (B9)$$

all the χ_i can be determined uniquely.

Proof of Lemma 1. We present a proof by contradiction: Let the $\{A_i\}_{i=1}^k$ be such that conditions (B8) and (B9) laid out in the lemma are satisfied. Suppose now that Equation (B8) does not uniquely determine all the $\chi_i \in \{-1,1\}$, that is, there exist some $\{j_1,\ldots,j_m\} \subset \{1,\ldots,k\}$ such that

$$\sum_{i \in \{1, \dots, k\} \setminus \{j_1, \dots, j_m\}} \chi_i A_i + \sum_{i \in \{j_1, \dots, j_m\}} \chi_i A_i = C$$
 (B10a)

and

$$\sum_{i \in \{1, \dots, k\} \setminus \{j_1, \dots, j_m\}} \chi_i A_i - \sum_{i \in \{j_1, \dots, j_m\}} \chi_i A_i = C .$$
 (B10b)

Then, deducting Equation (B10b) from Equation (B10a), we obtain

$$\sum_{i \in \{j_1, \dots, j_m\}} \chi_i A_i = 0 . \tag{B11}$$

Thus, we have found a partial sum of the products $\chi_i A_i$ that vanishes, which poses a contradiction to Equation (B9).

Lemma 2 (Adding a box to the first row of a Young diagram) Let α be a Young diagram and let M_1 and M^{11} be the diagrams obtained from α by adding one, respectively two, box(es) to the first row of α . Furthermore, let d_1 and d_{11} be the dimensions of the irreducible representations corresponding to M_1 and M^{11} , respectively. Then,

$$\frac{d_{11}}{d_1} = 1 \quad \Rightarrow \quad N \le 1 \ , \tag{B12}$$

where equality holds if and only if α is the totally symmetric diagram consisting of exactly one row.

Proof of Lemma 2. Let $h_{a,b}$ be the hook lengths (see Appendix E) of α , and denote by ℓ the length of α 's first row. We calculate d_{11}/d_1 using the factors-over-hooks formula (E2). For M^{11} , compared to M_1 , we obtain just one additional factor, namely $N + \ell + 1$ for the last box in the first row, and only the hook lengths for the boxes in the first row differ. In the quotient d_{11}/d_1 all other hook lengths cancel, i.e.

$$\frac{d_{11}}{d_1} = (N + \ell + 1) \frac{(h_{1,1} + 1)(h_{1,2} + 1)\cdots(h_{1,\ell} + 1)\cdot 1}{(h_{1,1} + 2)(h_{1,2} + 2)\cdots(h_{1,\ell} + 2)\cdot 2}.$$
(B13)

Hence,

$$d_{11}/d_1 = 1 \quad \Leftrightarrow \quad N = \frac{(h_{1,1} + 2)(h_{1,2} + 2)\cdots(h_{1,\ell} + 2)}{(h_{1,1} + 1)(h_{1,2} + 1)\cdots(h_{1,\ell} + 1)} \cdot 2 - \ell - 1.$$
 (B14)

The quotients $\frac{h_{1,b}+2}{h_{1,b}+1}$ are maximal if $h_{1,b}$ is minimal, and $h_{1,b} \ge \ell - b + 1$, where equality holds if and only if there is only one box in column b. Therefore,

$$N \le \frac{(\ell+2)(\ell+1)\cdots 3}{(\ell+1)\cdots 3\cdot 2}\cdot 2 - \ell - 1 = 1, \tag{B15}$$

as required.
$$\Box$$

Let's manipulate the linear relation (26d) a little bit: First, we single out the known value $S_{i,i}^{ii} = \frac{1}{d_i}$ from the sum,

$$1 = \sum_{b} d_{ib} S_{i,i}^{ib} = \frac{d_{ii}}{d_i} + \sum_{b \neq i} d_{ib} S_{i,i}^{ib} . \tag{B16}$$

We would like to view the signs of the 6j symbols as variables to be determined, and therefore define χ_{ij}

$$\chi_{ij} = \chi_{ji} \in \{-1, 1\} ,$$
(B17)

such that

$$S_{i,i}^{ij} = \chi_{ij} \frac{1}{d_i} \sqrt{1 - \frac{d_i d_j}{d_\alpha d_{ij}}} . \tag{B18}$$

Notice that χ_{ij} does not encompass the relative sign between $S_{i,i}^{ij}$ and $S_{j,j}^{ji}$ but denotes the absolute sign of $S_{i,i}^{ij}$. In other words,

$$S_{i,i}^{ij} = \chi_{ij} \frac{1}{d_i} \sqrt{1 - \frac{d_i d_j}{d_\alpha d_{ij}}} \xrightarrow{(32)} -\chi_{ij} \frac{1}{d_j} \sqrt{1 - \frac{d_i d_j}{d_\alpha d_{ij}}} = -\frac{d_j}{d_i} S_{j,j}^{ji} . \tag{B19}$$

Furthermore, to make the notation a bit shorter, let us define the symbol A_{ij} as

$$A_{ij} = \frac{d_{ij}}{d_i} \sqrt{1 - \frac{d_i d_j}{d_\alpha d_{ij}}} \qquad \Longrightarrow \qquad \chi_{ij} A_{ij} = d_{ij} S_{i,i}^{ij} . \tag{B20}$$

Clearly, the d_{ij} are symmetric in i and j, and so are the $S_{i,i}^{ij}$ in their upper indices by Equation (9), $S_{i,i}^{ij} = S_{i,i}^{ji}$. However, $S_{i,i}^{ij}$ and $S_{j,j}^{ij}$ are related by a negative pre-factor according to Equation (32) in Theorem 1, such that the A_{ij} are antisymmetric,

$$A_{ji} = -A_{ij} . (B21)$$

Then, taking $\frac{d_{ii}}{d_i}$ to the other side of the equal sign and implementing notation (B20), the linear equations in (B16) can be cast into matrix form,

$$\begin{pmatrix} 0 & \chi_{12}A_{12} & \chi_{13}A_{13} & \dots & \chi_{1N}A_{1N} \\ -\chi_{12}A_{12} & 0 & \chi_{23}A_{23} & \dots & \chi_{2N}A_{2N} \\ -\chi_{13}A_{13} & -\chi_{23}A_{23} & 0 & \dots & \chi_{3N}A_{3N} \\ \vdots & \vdots & \vdots & \ddots & \vdots \\ -\chi_{1N}A_{1N} & -\chi_{2N}A_{2N} & -\chi_{3N}A_{3N} & \dots & 0 \end{pmatrix} \begin{pmatrix} 1 \\ 1 \\ 1 \\ 1 \\ 1 \\ 0 \end{pmatrix} = \begin{pmatrix} 1 - \frac{d_{11}}{d_1} \\ 1 - \frac{d_{22}}{d_2} \\ 1 - \frac{d_{33}}{d_3} \\ \vdots \\ 1 - \frac{d_{NN}}{d_N} \end{pmatrix}.$$
(B22)

Recall that the A_{ij} are known (as the dimensions d_{α} , d_i , d_j and d_{ij} are known, cf. Equation (B20)) and that we seek to determine the $\chi_{ij} \in \{-1,1\}$ for each pair (i,j). We shall denote the linear equation resulting from row r of the matrix equation (B22) by E(r), that is:

$$E(r): -\sum_{i=1}^{r-1} \chi_{ir} A_{ir} + \sum_{j=r+1}^{N} \chi_{rj} A_{rj} = 1 - \frac{d_{rr}}{d_r}.$$
 (B23)

Notice that, up to this point, we have not specified a particular value for N but kept the discussion fully general. From now on, let us fix N = 3. (We note that the below argument also works for N < 3. At the end of this section, we comment on why the strategy presented here for determining the signs breaks down for N > 3.)

a. For N = 3, the matrix equation (B22) simplifies as

$$\begin{pmatrix} 0 & \chi_{12}A_{12} & \chi_{13}A_{13} \\ -\chi_{12}A_{12} & 0 & \chi_{23}A_{23} \\ -\chi_{13}A_{13} & -\chi_{23}A_{23} & 0 \end{pmatrix} \begin{pmatrix} 1 \\ 1 \\ 1 \end{pmatrix} = \begin{pmatrix} 1 - \frac{d_{11}}{d_1} \\ 1 - \frac{d_{22}}{d_2} \\ 1 - \frac{d_{33}}{d_3} \end{pmatrix}.$$
(B24)

From Lemma 2 we know that $\frac{d_{11}}{d_1} \neq 1$ for all N > 1, so, in particular, also for N = 3. Therefore, the right-hand side of E(1) is nonzero, which means that

$$A_{12} \neq A_{13}$$
 and not both A_{12} and A_{13} are zero. (B25)

We distinguish two cases:

- 1. If $A_{12} \neq 0$ and $A_{13} \neq 0$, then both χ_{12} and χ_{13} can be determined uniquely from E(1) by Lemma 1.
 - (a) If $A_{23} \neq 0$, we may also uniquely determine χ_{23} .
 - (b) If $A_{23} = 0$ for N = 3, the corresponding 6j symbols S_{22}^{23} and S_{33}^{23} both vanish and hence χ_{23} is irrelevant.
- 2. If only one of A_{12} and A_{13} is nonzero (i.e. only one of χ_{12} and χ_{13} can be determined uniquely), this means that the other 6j symbol is zero, making the corresponding χ_{ij} irrelevant. Without loss of generality, suppose that χ_{12} is uniquely determinable and hence $S_{11}^{13} = 0 = S_{33}^{13}$ (the analogous argument can be made if only χ_{13} is uniquely determinable).
 - (a) If $A_{23} \neq 0$, we may also uniquely determine χ_{23} from E(2) using our result for χ_{12} .
 - (b) If $A_{23} = 0$, the corresponding 6j symbols S_{22}^{23} and S_{33}^{23} both vanish, making χ_{23} irrelevant.

Therefore, for N = 3 all signs of the nonzero 6j symbols are uniquely determinable.

Let us briefly comment on possibly non-existing 6j symbols: Notice that, for a particular diagram α , boxes may be added only to the second row but not the third row (or vice versa), implying that the 6j symbols with an index 3 (resp. 2) do not exist. Examples of these are

$$\alpha = \square \square$$
 boxes can only be added in rows 1 and 2 (B26a)

$$\alpha = \square$$
 boxes can only be added in rows 1 and 3. (B26b)

Then, in both cases, the matrix equation (B24) reduces to something even simpler, namely

$$\begin{pmatrix} 0 & \chi_{1j} A_{1j} \\ -\chi_{1j} A_{1j} & 0 \end{pmatrix} \begin{pmatrix} 1 \\ 1 \end{pmatrix} = \begin{pmatrix} 1 - \frac{d_{11}}{d_1} \\ 1 - \frac{d_{jj}}{d_j} \end{pmatrix} \quad \text{where } j = 2 \text{ (resp. } j = 3) ,$$
 (B27)

and hence the signs of the only remaining 6j symbols S_{11}^{1j} and S_{jj}^{1j} can be determined from the sign of $1 - \frac{d_{11}}{d_1} \neq 0$.

b. Going beyond N = 3: Notice that for N = 3, each equation E(n) has exactly N-1 = 2 terms on the left-hand side. Since the right-hand side of E(1) is non-zero for all values of N, this, in particular, allows us to uniquely determine the sign of both terms of E(1) for N = 3, and thus also for one of the two terms appearing on the left-hand sides of E(2) and E(3), respectively. This is no longer the case for N > 3 as the left hand-sides of equations E(n) contain N-1 > 2 terms, and further information is needed to uniquely determine their signs.

Appendix C: Vertex properties

We discuss the behavior of vertices under line swapping. Consider three irreps α , β and γ with $\gamma^* \subset \alpha \otimes \beta$. For each instance of γ^* in $\alpha \otimes \beta$ we introduce — for the sake of argument — two vertices

$$\alpha \gamma \beta$$
 and $\beta \gamma \alpha$, (C1)

which differ by line ordering (and possibly other "internal" vertex structure). If the multiplicity of γ^* in $\alpha \otimes \beta$ is one (or, equivalently, if the multiplicity of β^* in $\alpha \otimes \gamma$ is one or, equivalently, if the multiplicity of α^* in $\beta \otimes \gamma$ is one), then the two vertices must be proportional

with some non-zero a priori complex constant c. All vertices appearing in this work have multiplicity one, as can be seen from Young diagram multiplication, using that in each vertex at least one line is in the fundamental representation.

Next, we consider the complex conjugates of both vertices, and temporarily introduce different symbols for them,

$$\begin{pmatrix} \alpha & \beta \\ \gamma & \end{pmatrix}^* = \begin{pmatrix} \alpha & \beta \\ \gamma & \end{pmatrix}^* = \begin{pmatrix} \beta & \alpha \\ \gamma & \end{pmatrix}^* = \begin{pmatrix} \alpha & \beta \\ \gamma & \end{pmatrix}^* . \tag{C3}$$

The complex conjugate of Equation (C2) reads

$$\beta \gamma = c^* \beta \gamma \alpha , \qquad (C4)$$

and we can use these two equations in order to relate two 3j symbols,

If we normalize all 3j symbols in the same way (we prefer to set them to 1, but the argument also works for any other normalization) then we conclude that |c| = 1. In fact, if $\alpha \neq \beta \neq \gamma \neq \alpha$, we can, and do, always choose c = 1, which is the most natural choice.

However, if two of the three irreps meeting in a vertex are equivalent, say $\beta = \alpha$, then the two vertices defined in Equation (C1) are proportional to each other, and we make the natural choice

$$\gamma = \gamma \alpha , \qquad (C6)$$

any other choice would give a redundant definition. In this case Equation (C2) becomes

$$\frac{\alpha}{\gamma} = c \frac{\alpha}{\gamma}, \qquad (C7)$$

and by intertwining the upper two lines in the last equation we also obtain

$$\gamma = c \gamma \qquad (C8)$$

Finally, dividing both sides with c, $c = \frac{1}{c}$, and we find $c = \pm 1$, i.e. we are left with a sign. In this work, the only irrep which can appear more than once in a vertex is the fundamental

representation, or, in other words, if two identical lines meet in a vertex then they are always quark-lines. Hence, there are only two vertices of this kind relevant for this work, one with c = 1 and one with c = -1,

warranting the use of the same symbol • for all vertices.

From here on, we again use the same symbol \bullet for both vertices \bullet and \blacksquare , an let the arrow direction determine which vertex is intended. We also no longer use the vertices \circ and \blacksquare but instead swap lines on the vertex \bullet . If an equation becomes more legible with two lines swapped in a vertex, we indicate this swapping of lines by a barred vertex (cf. Section IV A), i.e. we define

$$\beta \gamma \alpha = \beta \gamma \alpha , \qquad (C10)$$

and for the purpose of this work we only have to keep in mind that there is exactly one vertex, see Equation (C9), for which omitting a bar leads to a sign change.

Appendix D: Special cases for line ordering in vertices

In Appendix C we explained that we can largely ignore the line ordering in (barred) vertices of the 6j symbols, since for the 6j symbols we study most vertices connect three distinct irrep lines. The only exception are vertices with two incoming or two outgoing quark-lines, and among these vertices only the vertex

$$\Box$$

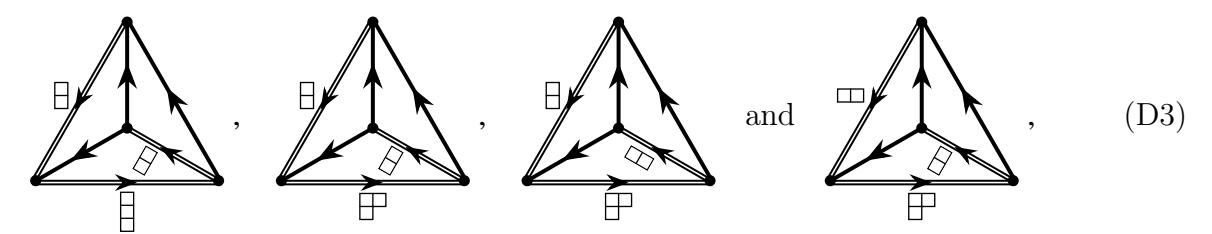
is antisymmetric in the two quark-lines, see Equation (C9).

In order to have two incoming or two outgoing quark-lines in a vertex within the 6j symbols under investigation,



 α or M_i or M_j needs to be the fundamental representation, i.e. a quark-line.

If $\alpha = \square$ then M_i and M_j can be either \square or \square , and the only 6js of this kind with at least one antisymmetric vertex are



which have all been explicitly discussed and calculated in Ref. 30.

If $M_i = \square$, then M^{ij} can be either \square or \square , from which it follows that also $M_j = \square$, and α can be either the trivial representation (singlet) or the adjoint representation (a gluon-line). If α is a singlet then the 6j symbol, up to normalization, reduces to a 3j symbol. If α is the adjoint representation, then the only 6j of this kind with at least one antisymmetric vertex is



which has also been calculated in Ref. 30; in fact, it also reduces, up to normalization, to a 3j by the Fierz identity.

Appendix E: Dimensions of Young diagrams

As is clear from Theorem 1, calculating the dimensions of the irreps contained in a 6j is imperative to calculating the values of the 6j symbols discussed in this paper. Therefore, we here recapitulate how to calculate these dimensions directly from the corresponding diagrams.

First, we present the factors-over-hooks formula without proof; proofs can be found in standard textbooks such as Refs. 36,38,39.

Consider a Young diagram λ . For each of its cells, we may define a *factor* and a *hook* length in the following way:

• the factor $f_{a,b}$ of the cell $c_{a,b} \in \lambda$ in the a^{th} row and the b^{th} column is defined as

$$f_{a,b} = b - a . (E1)$$

• the hook length $h_{a,b}$ of the cell $c_{a,b}$ is defined to be the number of cells to the right of $c_{a,b}$ plus the number of cells below $c_{a,b}$ plus 1 ($c_{a,b}$ itself).

Then, the dimension of the SU(N) irrep corresponding to the diagram λ is given by

$$\dim(\lambda) = \prod_{c_{a,b} \in \lambda} \frac{(N + f_{a,b})}{h_{a,b}} , \qquad (E2)$$

where the product runs over all cells $c_{a,b}$ in λ . Let us provide an example for illustration: Consider the Young diagram

$$\lambda =$$
 (E3)

Then, the factors and hook lengths of each of the cells are

such that the dimension of the irrep corresponding to λ is given by

$$\dim(\lambda) = \left[\frac{N}{7} \frac{(N+1)}{5} \frac{(N+2)}{2} (N+3) \right] \left[\frac{(N-1)}{4} \frac{N}{2} \right] \left[\frac{(N-2)}{3} (N-1) \right] [N-3] , \quad (E5)$$

which is zero for $N \leq 3$ and, for example, becomes 36 for N = 4.

In QCD, a general Fock space sector may contain fundamental, antifundamental and also adjoint factors. Young diagrams for irreps on such a sector reflect this by containing the following conglomerates of boxes,

fundamental: adjoint:
$$N-1 \left\{ \begin{array}{c} \\ \\ \\ \\ \\ \end{array} \right. \qquad N-1 \left\{ \begin{array}{c} \\ \\ \\ \\ \end{array} \right. \qquad (E6)$$

$$\dim = N \qquad \dim = N^2-1 \; ,$$

where the dimensions can be verified using the factors-over-hooks formula. For SU(N), a column of length N may be crossed out in the calculation of the dimension (as the hook lengths in this column will cancel with the factors at the end of the respective rows), but it

may be preferable to not go the route of first adding boxes that will ultimately be taken away. King⁴⁰ offers such a way in terms of back-to-back tableaux, where columns of length N-1 are represented as boxes that are added to the left of the given Young diagram. We will not review this method of multiplying diagrams and calculating the corresponding dimensions here but rather refer readers to the original source, Ref. 40.

REFERENCES

- ¹J. E. Paton and H.-M. Chan, "Generalized Veneziano model with isospin," Nucl. Phys. B **10**, 516–520 (1969).
- ²F. A. Berends and W. Giele, "The six gluon process as an example of Weyl-van der Waerden spinor calculus," Nucl. Phys. **B294**, 700 (1987).
- ³M. L. Mangano, S. J. Parke, and Z. Xu, "Duality and multi-gluon scattering," Nucl. Phys. B **298**, 653 (1988).
- ⁴M. L. Mangano, "The color structure of gluon emission," Nucl. Phys. B **309**, 461 (1988).
- ⁵D. A. Kosower, "Color factorization for fermionic amplitudes," Nucl. Phys. **B315**, 391–418 (1989).
- ⁶Z. Nagy and D. E. Soper, "Parton showers with quantum interference," JHEP **09**, 114 (2007), arXiv:0706.0017 [hep-ph].
- ⁷M. Sjodahl, "Color structure for soft gluon resummation a general recipe," JHEP **0909**, 087 (2009), arXiv:0906.1121 [hep-ph].
- ⁸J. Alwall, M. Herquet, F. Maltoni, O. Mattelaer, and T. Stelzer, "MadGraph 5: going beyond," JHEP **1106**, 128 (2011), arXiv:1106.0522 [hep-ph].
- ⁹M. Sjodahl, "ColorFull a C++ library for calculations in $SU(N_c)$ color space," Eur.Phys.J. C75, 236 (2015), arXiv:1412.3967 [hep-ph].
- 10 S. Plätzer and M. Sjodahl, "Subleading N_c improved parton showers," JHEP **1207**, 042 (2012), arXiv:1201.0260 [hep-ph].
- ¹¹S. Plätzer, M. Sjodahl, and J. Thorén, "Color matrix element corrections for parton showers," JHEP **11**, 009 (2018), arXiv:1808.00332 [hep-ph].
- ¹²G. 't Hooft, "A planar diagram theory for strong interactions," Nucl. Phys. **B72**, 461 (1974).
- ¹³A. Kanaki and C. G. Papadopoulos, "HELAC-PHEGAS: Automatic computation of

- helicity amplitudes and cross-sections," AIP Conf. Proc. 583, 169 (2002), arXiv:hep-ph/0012004.
- ¹⁴F. Maltoni, K. Paul, T. Stelzer, and S. Willenbrock, "Color flow decomposition of QCD amplitudes," Phys. Rev. D **67**, 014026 (2003), arXiv:hep-ph/0209271 [hep-ph].
- 15 S. Plätzer, "Summing large-n towers in colour flow evolution," Eur. Phys. J. C **74**, 2907 (2014), arXiv:1312.2448 [hep-ph].
- ¹⁶R. Ángeles Martínez, M. De Angelis, J. R. Forshaw, S. Plätzer, and M. H. Seymour, "Soft gluon evolution and non-global logarithms," JHEP **05**, 044 (2018), arXiv:1802.08531 [hep-ph].
- ¹⁷M. De Angelis, J. R. Forshaw, and S. Plätzer, "Resummation and simulation of soft gluon effects beyond leading color," Phys. Rev. Lett. **126**, 112001 (2021), arXiv:2007.09648 [hep-ph].
- ¹⁸S. Plätzer and I. Ruffa, "Towards colour flow evolution at two loops," JHEP **06**, 007 (2021), arXiv:2012.15215 [hep-ph].
- ¹⁹S. Keppeler and M. Sjodahl, "Orthogonal multiplet bases in $SU(N_c)$ color space," JHEP **09**, 124 (2012), arXiv:1207.0609 [hep-ph].
- 20 A. Kyrieleis and M. H. Seymour, "The colour evolution of the process $qq\to qqg$," JHEP **01**, 085 (2006), hep-ph/0510089.
- ²¹Y. L. Dokshitzer and G. Marchesini, "Soft gluons at large angles in hadron collisions," JHEP **01**, 007 (2006), arXiv:hep-ph/0509078.
- $^{22}\text{M}.$ Sjodahl, "Color evolution of 2 \rightarrow 3 processes," JHEP **12**, 083 (2008), arXiv:0807.0555 [hep-ph].
- ²³M. Beneke, P. Falgari, and C. Schwinn, "Soft radiation in heavy-particle pair production: All-order colour structure and two-loop anomalous dimension," Nucl. Phys. B 828, 69–101 (2010), arXiv:0907.1443 [hep-ph].
- ²⁴Y.-J. Du, M. Sjodahl, and J. Thorén, "Recursion in multiplet bases for tree-level MHV gluon amplitudes," JHEP **05**, 119 (2015), arXiv:1503.00530 [hep-ph].
- ²⁵M. Sjodahl and J. Thorén, "Decomposing color structure into multiplet bases," JHEP 09, 055 (2015), arXiv:1507.03814 [hep-ph].
- ²⁶S. Keppeler and M. Sjodahl, "Hermitian Young operators," J. Math. Phys. **55**, 021702 (2014), arXiv:1307.6147 [math-ph].
- $^{27}\mathrm{J}.$ Alcock-Zeilinger and H. Weigert, "Simplification rules for birdtrack operators," J. Math.

- Phys. 58, 051701 (2017), arXiv:1610.08801.
- ²⁸J. Alcock-Zeilinger and H. Weigert, "Compact Hermitian Young projection operators," J. Math. Phys. 58, 051702 (2017), 1610.10088.
- ²⁹J. Alcock-Zeilinger and H. Weigert, "Transition operators," J. Math. Phys. **58**, 051703 (2017), arXiv:1610.08802 [math-ph].
- ³⁰M. Sjodahl and J. Thorén, "QCD multiplet bases with arbitrary parton ordering," JHEP 11, 198 (2018), arXiv:1809.05002 [hep-ph].
- ³¹H. T. Johansson and C. Forssén, "Fast and accurate evaluation of Wigner 3*j*, 6*j*, and 9*j* symbols using prime factorization and multiword integer arithmetic," SIAM Journal on Scientific Computing **38**, A376–A384 (2016).
- 32 A. Alex, M. Kalus, A. Huckleberry, and J. von Delft, "A numerical algorithm for the explicit calculation of SU(n) and SL(n,c) Clebsch-Gordan coefficients," Journal of Mathematical Physics **52**, 023507 (2011).
- ³³T. Dytrych, D. Langr, J. P. Draayer, K. D. Launey, and D. Gazda, "SU3lib: A C++ library for accurate computation of Wigner and Racah coefficients of SU(3)," Comput. Phys. Commun. **269**, 108137 (2021).
- ³⁴S. Gieseke, P. Kirchgaeßer, S. Plätzer, and A. Siodmok, "Colour reconnection from soft gluon evolution," JHEP **11**, 149 (2018), arXiv:1808.06770 [hep-ph].
- ³⁵S. Plätzer, "Colour evolution and infrared physics," (2022), arXiv:2204.06956 [hep-ph].
- ³⁶P. Cvitanović, *Group theory: Birdtracks, Lie's and exceptional groups* (Princeton Univ. Pr., USA: Princeton, 2008).
- ³⁷S. Keppeler, "Birdtracks for SU(N)," SciPost Phys. Lect. Notes **3**, 1 (2018), arXiv:1707.07280 [math-ph].
- $^{38}\mathrm{W.}$ Fulton, Young Tableaux (Cambridge Univ. Pr., UK: Cambridge, 1997).
- ³⁹B. E. Sagan, The Symmetric Group Representations, Combinatorical Algorithms, and Symmetric Functions, 2nd ed. (Springer, USA: New York, 2000).
- ⁴⁰R. C. King, "Generalized Young tableaux and the general linear group," J. of Math. Phys. **11**, 280–293 (1970).